Supplementary Tables

Supplementary Table 1. Data collection and refinement statistics for selenomethionine labeled protein

		Dbp5-CTD^{L327V}/ IP$_6$/Gle1^{H337R}		Dbp5-CTD^{L327V}/ IP$_6$/Gle1^{WT}
Data collection				
Space group		$P6_122$		$P6_122$
Cell dimensions				
a, *b*, *c* (Å)		110.4, 110.4, 201.5		110.9, 110.9, 201.9
α, β, γ (º)		90.0, 90.0, 120		90.0, 90.0, 120
	Peak	*Inflection*	*Remote*	*Remote*
Wavelength	0.9796	0.9798	1.020	1.116
Resolution (Å)	50-2.7 (2.8-2.7)	50-2.8 (2.9-2.8)	50-2.6 (2.7-2.6)	50-2.5 (2.6-2.5)
R_{sym} or R_{merge}	12.9 (74.6)	12.5 (63.1)	10.0 (69.0)	9.4 (47.8)
$I/\sigma I$	21.7 (3.8)	24.9 (5.3)	18.9 (2.8)	20.1 (2.5)
Completeness (%)	100 (100)	100 (100)	99.9 (100)	99.3 (94.0)
Redundancy	15.5 (15.2)	16.7 (16.8)	7.5 (7.4)	7.5 (4.1)
Refinement				
Resolution (Å)		48-2.6		48-2.5
No. reflections		39,606		25,940
R_{work}/ R_{free}		18.7 / 21.3[a]		20.2 / 23.8[a]
No. atoms				
Protein		3808		3807
Ligand/ion		59		59
Water		57		80
B-factors				
Protein		58.2		61.2
Ligand/ion		65.7		65.0
Water		49.5		50.1
R.m.s deviations				
Bond lengths (Å)		0.003		0.004
Bond angles (º)		0.677		0.708

*Highest resolution shell is shown in parenthesis.

[a] R_{free} is calculated using 5% of the data omitted from refinement

Supplementary Table 2. Data collection and refinement statistics for native protein

	Δ90Dbp5^{L327V}/ IP$_6$/Gle1^{H337R}/ ADP	Δ90Dbp5^{L327V}/ RNA/ ADP•BeF$_3$	Δ90Dbp5/ RNA/ ADP•BeF$_3$	Δ90Dbp5^{L327V}/ IP$_6$/Gle1^{H337R}/ ADP/Nup159
Data collection				
Space group	$I2_13$	$P2_12_12_1$	$P2_12_12_1$	C2
Cell dimensions				
a, *b*, *c* (Å)	207.0, 207.0, 207.0	42.31, 90.81, 105.1	42.14, 92.21, 104.5	186.9, 67.98, 132.4
α, β, γ (°)	90.0, 90.0, 90.0	90.0, 90.0, 90.0	90.0, 90.0, 90.0	90.0, 128, 90.0
Resolution (Å)	104-4.0 (4.2-4.0)	50-1.5 (1.6-1.5)	50-1.4 (1.5-1.4)	50-2.9 (3.0-2.9)
R_{sym} or R_{merge}	9.1 (61.7)	6.2 (32.8)	4.0 (43.5)	10.1 (66.8)
$I/\sigma I$	12.7 (3.2)	25.1 (3.5)	26.2 (2.3)	12.6 (2.0)
Completeness (%)	100 (100)	98.8 (97.7)	94.0 (67.0)	99.8 (99.7)
Redundancy	7.0 (7.2)	6.9 (3.9)	3.6 (2.3)	3.7 (3.5)
Refinement				
Resolution (Å)	103-4.0	34-1.5	45-1.4	48-2.9
No. reflections	12,612	64,601	75, 947	29,959
R_{work}/ R_{free}	21.4 / 23.9[b]	16.5 / 18.9[a]	16.0 / 18.0[a]	22.9 / 26.2[a]
No. atoms				
Protein	5442	3252	3318	8259
Ligand/ion	135	160	162	64
Water	0	532	493	0
B-factors				
Protein	158	15.6	14.5	61.1
Ligand/ion	205	20.6	19.5	82.9
Water	-	28.8	27.8	-
R.m.s deviations				
Bond lengths (Å)	0.007	0.013	0.016	0.002
Bond angles (°)	0.556	1.503	1.516	0.532

*Highest resolution shell is shown in parenthesis.

[a] R_{free} is calculated using 5% of the data omitted from refinement

[b] R_{free} is calculated using 10% of the data omitted from refinement

Supplementary Table 3. Binding and release values for MANT nucleotides and RNA.

	DQAD mutant	**WT**
MANT-ADP release	k_{off}	k_{off}
Dbp5	0.29 +/- 0.02 s^{-1}	n.d.
Dbp5 + Gle1 + IP_6	0.26 +/- 0.03 s^{-1}	n.d.
Dbp5 + RNA	0.26 +/- 0.02 s^{-1}	n.d.
Dbp5 + RNA + Gle1 + IP_6	0.23 +/- 0.02 s^{-1}	n.d.
MANT-ADP binding	Kd	Kd
Dbp5	150 +/- 22 nM	n.d.
Dbp5 + Gle1 + IP_6	142 +/- 34 nM	n.d.
RNA binding (29 nt ssRNA)	Kd	Kd
Dbp5 + ATP	70 +/- 30 nM	n.d.
Dbp5 + ATP + Gle1 + IP_6	67 +/- 27 nM	280 +/- 27 nM
Δ90Dbp5 + ATP	n.d.	207 +/- 15 nM
Δ90Dbp5 + ATP + Gle1 + IP_6	n.d.	384 +/- 90 nM
RNA release (29 nt ssRNA)	k_{off}	k_{off}
Dbp5 + ATP	0.0039 +/- 0.0003 s^{-1}	n.d.
Dbp5 + ATP + Gle1 + IP_6	0.033 +/- 0.009 s^{-1}	0.28 +/- 0.014 s^{-1}
Dbp5 + ATP + Gle1$^{VAI \rightarrow DDD}$ + IP_6	0.0042 +/- 0.012 s^{-1}	n.d.
RNA release (25 nt ssRNA)	k_{off}	k_{off}
eIF4A + ATP	0.0186 +/- 0.003 s^{-1}	n.d.
eIF4A + ATP + eIF4G	0.091 +/- 0.03 s^{-1}	n.d.

n.d. = not determined

Supplementary Table 4. Yeast Strain List

Strain	Genotype	Source or Reference
KWY1561	[*MAT***a**, *ura3-52*, *lys2-801*, *ade2-101*, *trp1-1*, *his3-200*, *leu2-1*, *gle1::KanMX6*, (pKW1718)]	[1]

Supplementary Table 5. Plasmid List

Plasmid	Description	Source or Reference
pKW1818	*GLE1/CEN/LEU2*	[1]
pKW2571	*GLE1/CEN/LEU2* (V513D/A516D/I520D)	This study
pKW1718	*GLE1/CEN/URA3*	This study
pKW1329	pSV271-DBP5	[1]
pKW1459	pSV271-NUP159 (2-387)	[2]
pKW2446	pSV271-DBP5 (E240Q)	This study
pKW2554	pSV271-DBP5 (K477A, K481A)	This study
pKW2496	pSV271-*DBP5-1*^{D} (267-482)	This study
pKW2499	pSV271-*DBP5-1*^{D} (91-482)	This study
pKW1716	pSV272-GLE1 (244-538)	[1]
pKW2570	pSV272-GLE1 (244-538) (V513D/A516D/I520D)	This study
pKW2456	pSV272-*GLE1-22*^{D} (244-538)	This study
pKW2625	pSV271-eIF4A (E172Q)	This study
pKW2613	pSV272-eIF4G (572-952)	This study

Supplementary figures

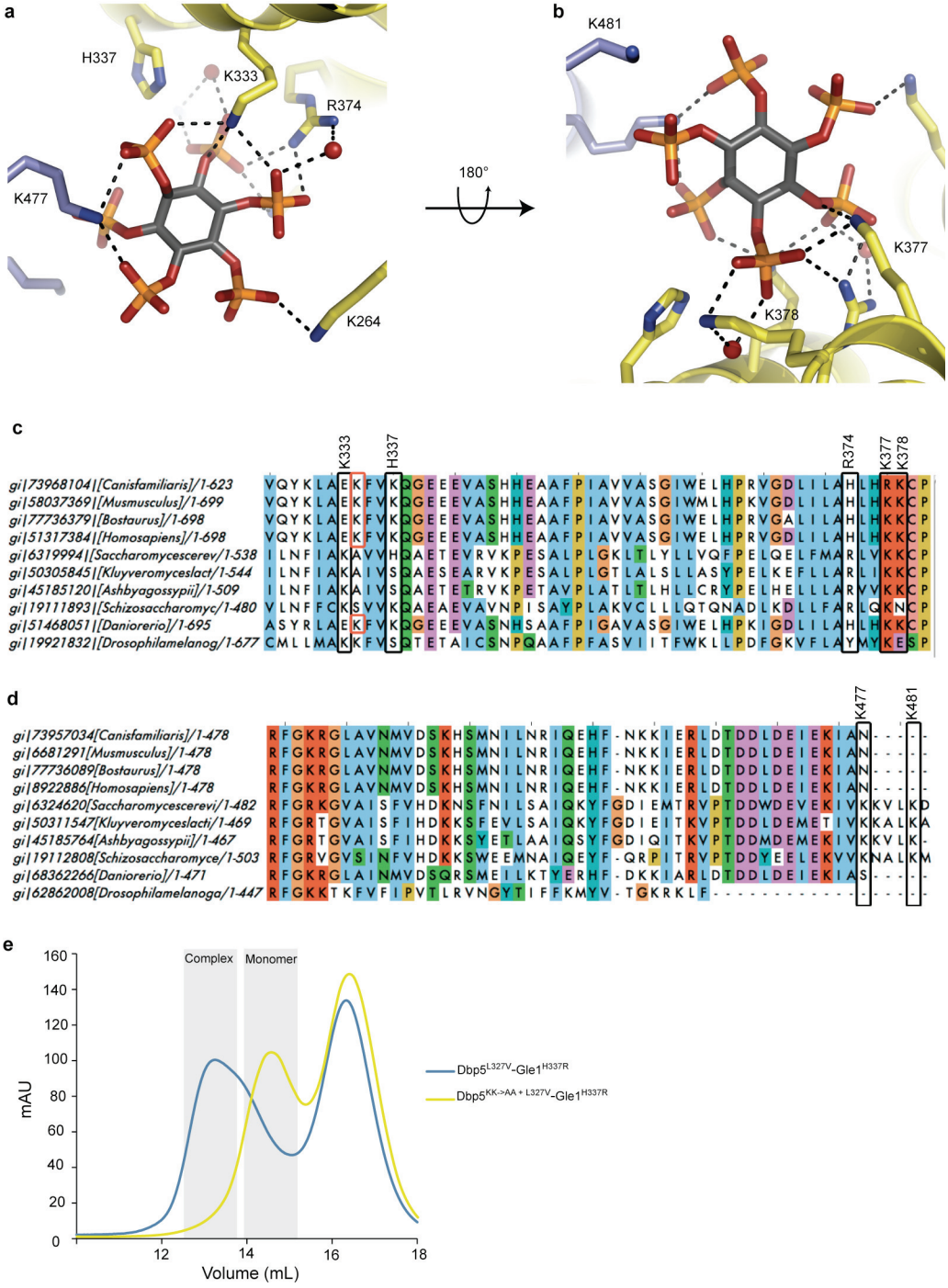

Supplementary Figure 1. Critical side chains required for IP_6 binding. a, b, Two views of the IP_6 binding pocket illustrating salt-bridging contacts between positively charged sidechains and the six phosphate groups of IP_6. Gle1 is depicted in yellow, Dbp5 in blue. **c, d.** Sequence conservation of eukaryotic Gle1 (**c**) and Dbp5 (**d**) homologues. While there is a lack of strict conservation among IP_6 binding residues beyond K377 and K378 in Gle1[3], polar residues capable of binding phosphate groups appear to be conserved at most sites. K377 and K378 make

three direct IP_6 contacts and one water-mediated contact in our structure (**b**), accounting for 4 of the 13 side chain-mediated polar contacts (~30%) with IP_6. These residues likely define the IP_6 binding core, whereas the other more variable residues may serve to tune IP_6 sensitivity in various species. In species where residue K333 has been changed to a residue of the opposite charge (K to E), there is a corresponding mutation of residue 334 to a lysine that may be capable of binding IP_6 . Alignments made using ClustalW[4]. **e,** $Dbp5^{KK->AA+L327V}$ does not form a stable complex with $Gle1^{H337R}$ by gel filtration. Elution profiles of $Dbp5^{L327V}$ or $Dbp5^{KK->AA+L327V}$ after mixing with $Gle1^{H337R}$ from a Superdex 200 gel filtration column in the presence of IP_6. The peak at ~16.5mL corresponds to cleaved His_6-MBP tag present in the Gle1 protein preparation.

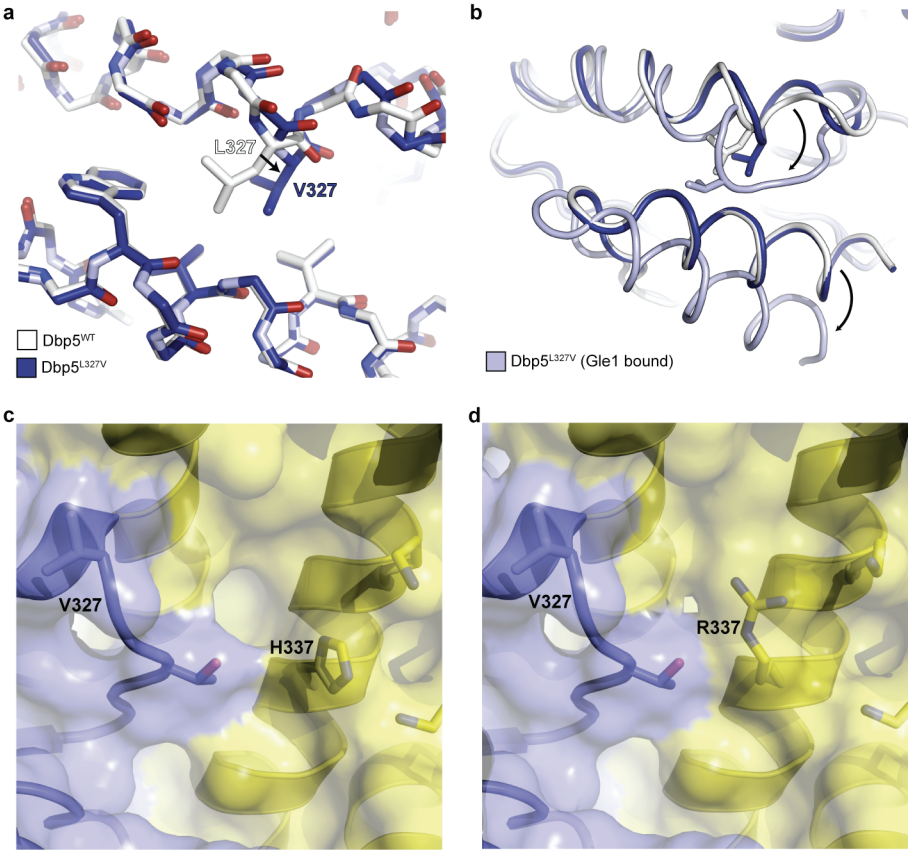

Supplementary Figure 2. Structural affects of $Dbp5^{L327V}$ and $Gle1^{H337R}$ gain-of-function mutations. a, A structural superposition of Δ90Dbp5-RNA structures in the presence and absence of the L327V mutation (see colour key). Change in side chain packing due to the gain-of-function mutation disrupts the structure of an α-helix in Dbp5. **b,** Superposing the structures in (**a**) onto the Δ90Dbp5-Gle1 structure (see colour key) reveals that the same alpha helix must bend to accommodate Gle1 binding. Thus, the disruption caused by V327 may lower the free energy for such a conformational change and stabilize the protein-protein complex. **c,** H337 lies within the IP_6 binding pocket at the Dbp5-Gle1 interface, but does not make any direct contacts with IP_6 (Supplementary Fig. 1a). Protein subunits coloured as in Figure 1. **d,** The H337R

mutation appears to contribute additional polar and van der Waals contacts to the Gle1-Dbp5 interface. The close vicinity of the V327 and R337 mutations at the protein-protein interface likely explains their cooperative effect in stabilizing the Dbp5-Gle1 complex (Supplementary Fig. 1e). Protein subunits coloured as in Figure 1.

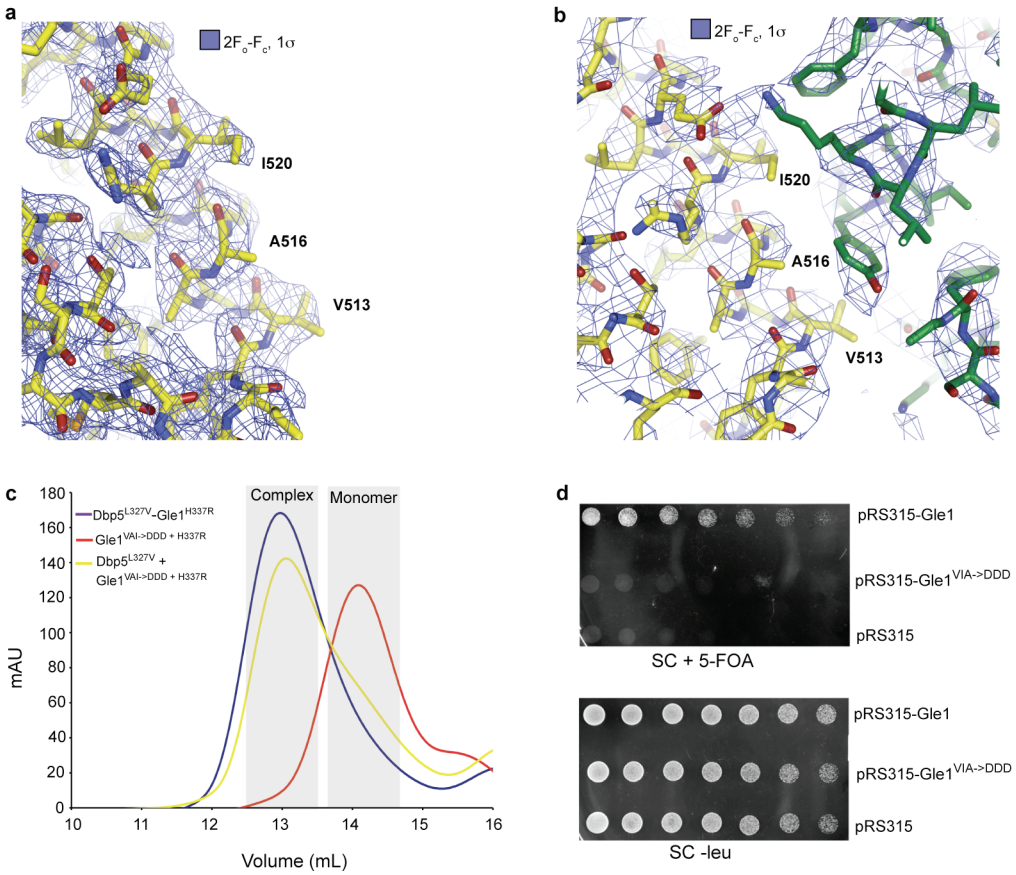

Supplementary Figure 3. Mutational analysis of the Gle1-Dbp5-NTD contact. a, Final refined $2F_o$-F_c electron density maps contoured at 1σ for the $Gle1^{WT}$-$Dbp5^{L327V}$ structure highlighting the solvent exposed hydrophobic residues V513, A516, and I520 on the C-terminal helix in Gle1. **b,** Final refined $2F_o$-F_c electron density maps contoured at 1σ for the $Gle1^{H337R}$-Δ90Dbp5 structure highlighting the Gle1-Dbp5-NTD interface. **c,** $Dbp5^{L327V}$ and $Gle1^{VAI->DDD+H337R}$ form a stable complex. Elution profiles of $Gle1^{VAI->DDD+H337R}$ or $Gle1^{H337R}$ in complex with $Dbp5^{L327V}$ compared to $Gle1^{VAI->DDD+H337R}$ alone. Elution profiles from a Superdex 200 gel filtration column in the presence of 30 mM HEPES (pH 7.5), 150 mM NaCl, 1 mM DTT, 0.25 mM IP_6, and 5% glycerol are shown. **d,** Dbp5-NTD/Gle1 contact is essential *in vivo*. Growth of KWY1561 carrying the indicated plasmids after one day of growth on SC + 5-FOA at 30°C.

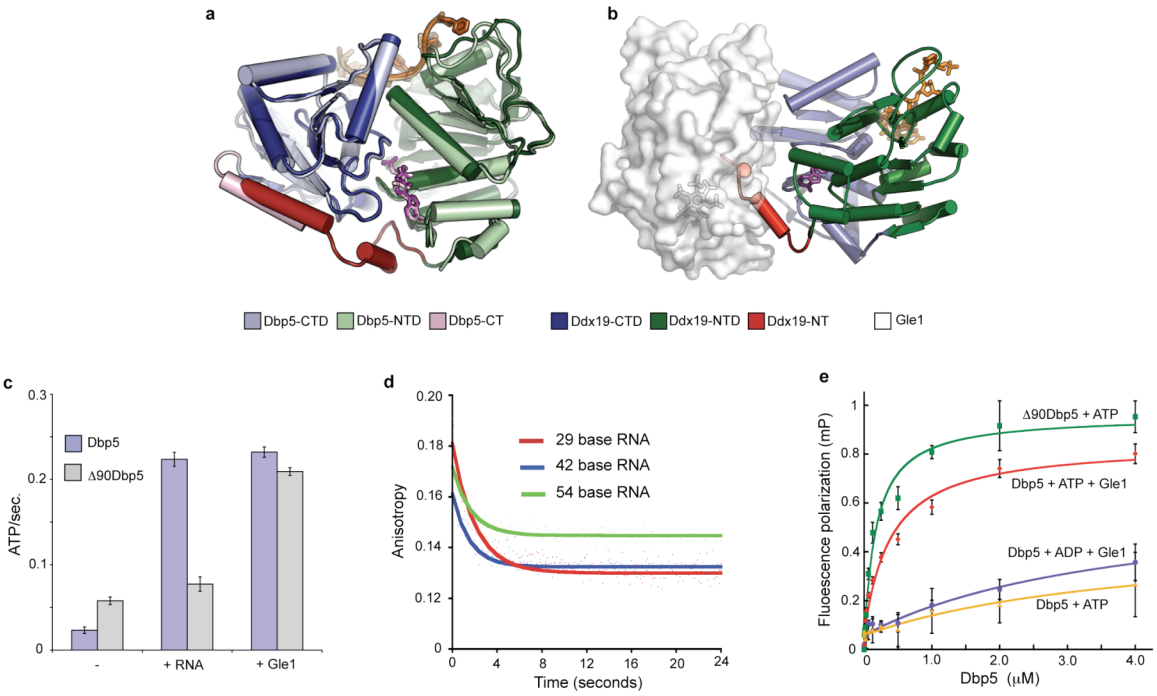

Supplementary Figure 4. Gle1 binding relieves Dbp5 auto-inhibition. a, Structural superposition of the RNA-Δ90Dbp5 complex bound to ADP•BeF_3 with the RNA-Ddx19 complex bound to AMP-PNP (PDB ID: 3G0H)[5] reveals nearly identical conformations of the two proteins. Note that the C-terminal helix required for IP_6 binding (pink) packs along the same surface as the N-terminal extension (red) present in the Ddx19 structure. **b,** Superposition of the RNA-Ddx19 complex with the Gle1-Δ90Dbp5 complex shows that the Ddx19 N-terminus (red) would clash with Gle1. **c,** Stimulation of Δ90Dbp5 ATPase activity by Gle1 suggests that Gle1 functions to relieve Dbp5 auto-inhibition. Error bars represent standard deviation (n=3). **d,** Dbp5 undergoes single turnover binding reactions with RNA. RNA release from Dbp5 was monitored by fluorescent polarization. Dbp5 (0.5μM), FITC-RNA (20nM), ATP (1mM), and Gle1 (1.0μM) were pre-mixed to allow steady state complex formation and then poly-A RNA (0.5mg/mL) was added by mixing in a stopped-flow chamber. Release measurements were made for ssRNA of lengths 29 ($t_{1/2}$ = 0.41 +/- 0.02 sec^{-1}), 42 ($t_{1/2}$ = 0.46 +/- 0.02 sec^{-1}), and 54 ($t_{1/2}$ = 0.47 +/- 0.06 sec^{-1}) bases. $t_{1/2}$ values are an average of three independent experiments +/- s.d. (n=3). Data were fit to a single exponential decay curve using KaleidaGraph (Synergy Software). Representative curves are shown for each condition. $t_{1/2}$ values correspond to a k_{off} of 0.28 to 0.33 s^{-1} which fits with a single turnover event given the measured ATPase rates under the same conditions (0.32 +/- 0.02 ATP sec^{-1}). **e,** RNA binding monitored by fluorescent polarization in the presence of IP_6 and ATP with Dbp5. Measured apparent K_d for Dbp5 + Gle1 was 280 +/- 27 nM, while Δ90Dbp5 was 207 +/- 15 nM (average +/- s.d. , n=3).

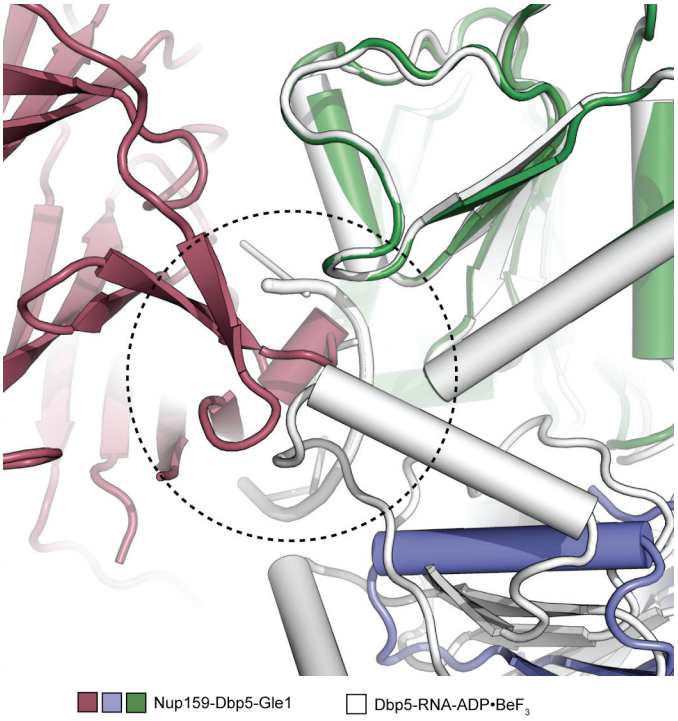

Supplementary Figure 5. Nup159 binding occludes the Dbp5 RNA binding site. A structural superposition of the Dbp5-RNA and Nup159-Dbp5-Gle1 structures shows that Nup159 sterically clashes (see dashed circle) with both the C-terminal RecA-like domain and the bound RNA in the closed ADP•BeF_3 bound state of Dbp5 (see colour key).

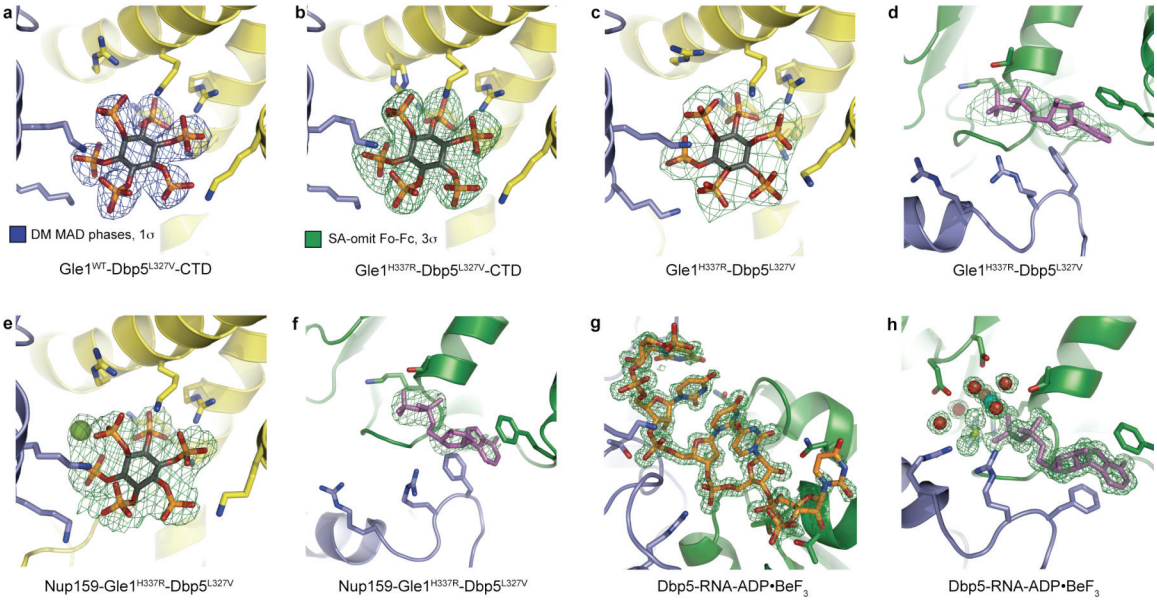

Supplementary Figure 6. Clear electron density is present for all ligands in the various structures. Gle1 is depicted in yellow, Dbp5-NTD in green and Dbp5-CTD in blue. **a,** Density-modified (DM), experimentally phased electron density maps shown at a contour level of 1σ for

IP_6 in the $Gle1^{H337R}$-$Dbp5^{L327V}$-CTD structure. The remaining panels show simulated annealing (SA) F_o-F_c omit maps contoured at 3σ calculated for all ligands. **b,** IP_6 in the $Gle1^{WT}$-$Dbp5^{L327V}$-CTD structure. **c,** IP_6 in the $Gle1^{H337R}$- Δ90$Dbp5^{L327V}$ structure. A B-factor sharpening value of -100 $Å^2$ was applied in order to more strongly weight high resolution data and improve the 4 Å electron density maps. **d,** ADP in the $Gle1^{H337R}$- Δ90$Dbp5^{L327V}$ structure. A B-factor sharpening value of -100 $Å^2$ was applied as in panel (**c**). **e,** IP_6 in the Nup159-$Gle1^{H337R}$- Δ90$Dbp5^{L327V}$ structure. **f,** ADP in the Nup159-$Gle1^{H337R}$- Δ90$Dbp5^{L327V}$ structure. **g,** RNA in the RNA-Δ90Dbp5 structure. **h,** ADP•BeF_3•Mg^{2+} and bound water molecules in the RNA-Δ90Dbp5 structure.

Supplementary References:

1. Weirich, C. S. *et al*. Activation of the DExD/H-box protein Dbp5 by the nuclear-pore protein Gle1 and its coactivator InsP6 is required for mRNA export. *Nat. Cell Biol.* **8**, 668-676 (2006).
2. Weirich, C. S., Erzberger, J. P., Berger, J. M. & Weis, K. The N-terminal domain of Nup159 forms a beta-propeller that functions in mRNA export by tethering the helicase Dbp5 to the nuclear pore. *Mol. Cell* **16**, 749-760 (2004).
3. Alcazar-Roman, A. R., Bolger, T. A. & Wente, S. R. Control of mRNA export and translation termination by inositol hexakisphosphate requires specific interaction with Gle1. *J. Biol. Chem.* (2010).
4. Larkin, M. A. *et al*. Clustal W and Clustal X version 2.0. *Bioinformatics* **23**, 2947-2948 (2007).
5. Collins, R. *et al*. The DEXD/H-box RNA helicase DDX19 is regulated by an {alpha}-helical switch. *J. Biol. Chem.* **284**, 10296-10300 (2009).